Journal of
Mechanical
Science and
Technology

Journal of Mechanical Science and Technology 21 (2007) 1331~1337

Drag Force Control of Flow over Wavy Cylinders at Low Reynolds Number

K. Lam*, Y. F. Lin

Department of Mechanical Engineering, The Hong Kong Polytechnic University, Hung Hom, Kowloon, Hong Kong

(Manuscript Received November 17, 2006; Revised May 2, 2007; Accepted May 26, 2007)

Abstract

Three-dimensional numerical simulations on the laminar flow around a circular cylinder with different diameter along the spanwise leading to a type of sinusoidal waviness, named wavy cylinder are performed at low Reynolds number. A series of wavy cylinders with different combinations of spanwise wavelength and wave amplitude are conducted at a Reynolds number of 100. The optimal range of wavelength and the effect of wave amplitude are obtained. The results show that the 3-D free shear layers from the cylinder are more difficult to roll up to vortex and hence the wake formation lengths of some typical wavy cylinders are larger than that of the circular cylinder and in some cases the free shear layers even do not roll up into vortex behind the cylinder. The mean drag coefficients of the typical wavy cylinders are less than that of a corresponding circular cylinder with the same mean diameter; also the fluctuating lift coefficients are reduced. The reduction of mean drag coefficient and fluctuating lift coefficient of wavy cylinder increases with the value of wavy amplitude. Furthermore, a typical wavy cylinder model at Re=150 is also simulated and found that the control of flow induced vibration by modifing the spanwise wavelength of cylinder has a relationship with the variation of Reynolds number.

Keywords: Wavy cylinders; Drag reduction; Low Reynolds number; Vortex structures

1. Introduction

Flow induced vibration (FIV) around cylindrical bluff bodies is a common problem in the general area of fluid-structure interaction. It includes many complex phenomena. The alternate vortices shedding from these bluff bodies generate oscillation effects which will give rise to the bluff body vibration and drag force generation. How to well control the vortices shedding is a challenging problem in the area drag reduction and FIV suppression. Over the past few years, many experimental investigations have been carried out on flow around different cylindrical bodies such as (Tombazis and Bearman, 1997; Bearman and Owen, 1998; Owen et al., 2000; Owen et al., 2001). Darekar and Sherwin numerically investigated the flow past a square cylinder with a wavy stagnation face at low Reynolds numbers (Darekar and Sherwin, 2001). The steady nature of the near wake is associated with a reduction in total drag of about 16% at a Reynolds number of 100 compared with the straight, non-wavy square cylinder. They showed that the unsteady and staggered Kármán vortex wake could be suppressed into a steady and symmetric structure due to the waviness of the square cylinder. They also suggested that the introduction of a span-wise waviness at a wavelength close to the mode-A spanwise wavelength and the primary streamwise wavelength of the flow behind the straight square cylinder would lead to the suppression of the Kármán street with a minimal input amplitude.

Based on the geometric disturbance ideas, a

*Corresponding author. Tel.: +852 2766 6649, Fax.: +852 2365 4703
E-mail address: mmklam@polyu.edu.hk

circular cylinder with different diameter along the spanwise, named wavy cylinder has been studied. In the experimental area, Ahmed et al. experimentally investigated the surface-pressure distributions of wavy cylinders with different spanwise wavelengths and the turbulent wake behind a wavy cylinder (Ahmed and Bays-Muchmore, 1992; Ahmed et al., 1993). But the drag reduction and suppression of vibration were not discussed. Lam et al. investigated the relation between the wave spanwise length of wavy cylinders and drag force by measuring aerodynamic forces using a load cell and pressure distributions (Lam et al., 2004a; Lam et al., 2004b). They found that drag reduction of up to 20% could be achieved by adjusting the amplitude and wave length of the cylinder at the range of Reynolds numbers from 20,000 to 50,000. Furthermore, they also found that the wavy geometry played an important role on vortex formation length which has a strong relation with the effect of drag reduction and vortex shedding suppression. The vortex formation length of the wavy cylinder is longer than that of the circular cylinder. It gives rise to the reduction of the drag force. At the nodal and saddle plane, the streamwise velocity distributions are very different compared with a circular cylinder. Flow visualization studies were also carried out at lower Reynolds number to visualize the vortex structure. Nguyen et al. investigated the near wake behind a wavy cylinder. A drag reduction up to 22% at the Reynolds number of 10,000 was obtained (Nguyen and Jee, 2004). Also they also showed that the longer vortex formation region of the wavy cylinder seems to be related with drag reduction. At the same Reynolds numbers, the vortex formation length is longer and the turbulent intensity is smaller than the circular cylinder. Recently, Zhang et al. (2005) investigated the three-dimensional near wake structures behind a wavy cylinder by using particle image velocimetry (PIV) technique at the Reynolds number of 3000 (Zhang et al., 2005). Along the span of wavy cylinder, well-organized streamwise vortices with alternating positive and negative vorticity were observed. They suppress the formation of the large-scale spanwise vortices and decrease the overall turbulent kinetic energy in the near wake of the wavy cylinder. The wavy surface geometry significantly modifies the near wake structure and strongly controls the 3D vortices formed in the near wake.

All the researches above are only set at a small region of the wavelength along the spanwise direction, while the optimal range of wavelength which can well suppress the vortex was not found. Furthermore, the amplitude of the wave line also plays an important role in control the vortex shedding from the wavy cylinders. And the three-dimensional vortices structures can not be illustrated clearly. In present study, we focus on investigating the three-dimensional vortex structures behind different wavy cylinders at the low Reynolds number by numerical method which can well capture the three dimensional vortex structures and all other instantaneous valuable data, such as drag, lift, pressure and velocity etc. The relationship between spanwise wavelength, wave amplitude and force coefficients will be investigated. The optimal range of the wave length will be obtained and also the three-dimensional vortex structures will be captured.

2. Geometry models

The geometry of the wavy cylinders can be described by the equation, $D = D_m + 2a\cos(2\pi z/\lambda)$. Figure 1 shows the schematic diagram of the wavy cylinder, where D is the local diameter of the wavy cylinder along the spanwise direction, the mean diameter is defined with $D_m = (D_{max} + D_{min})/2$, '$a$' is the amplitude of the surface curve, 'λ' is the wavelength along the spanwise direction and 'z' is the spanwise location. As shown in Fig.1, the axial locations (spanwise locations) with maximum local diameter are referred to 'nodes', while the axial locations of the minimum diameter are denoted 'saddles'

3. Numerical method

In present study the finite volume method (FVM) applied on unstructured grids is employed to calculate the incompressible unsteady Navier-Stokes equations. The governing equations can be written in vector form as

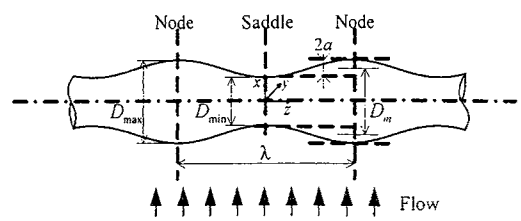

Fig. 1. Geometry of wavy cylinder models.

$$\frac{\partial u}{\partial t}+u\cdot\nabla u=-\nabla p+\frac{1}{\mathrm{Re}}\nabla^2 u \quad (1)$$

$$\nabla\cdot u=0 \quad (2)$$

where Re is the Reynolds number, Re=$U_\infty D_m/\nu$. U_∞ is the oncoming flow velocity, ν is the fluid kinematics viscosity, u is the non-dimensional flow velocity vector in the Cartesian coordinate system (x, y, z) with its three velocity components u, v and w, and p is the non-dimensional static pressure. The well known SIMPLE algorithm was used to deal with the pressure velocity coupling between the momentum and the continuity equations. The computational domain used for the simulations was set at $24D_m\times 32D_m\times\lambda$. The velocity at upstream boundary of the computational domain is set $12D_m$ away from the centre line of cylinders, while the convective outflow boundary condition is used at the outflow boundary. A periodic boundary condition is employed in the spanwise direction. And no-slip boundary condition is prescribed at the surface of cylinders. The lateral surfaces are treated as slip surfaces using symmetry conditions. In order to obtain the governing equations and different quantities in the non-dimensional form, the solution variables are normalized. All the parameters such as drag and lift coefficient, geometrical lengths, etc are scaled with D_m.

Table 1. Grid independent test together with other results of a circular cylinder at Re=100.

Test	Circum ference	Grid numbers	$\bar{C}_D$	C_L'	St	-C_{pb}
Present case 1	100	571200	1.340	0.234	0.165	0.726
Present case 2	120	649600	1.339	0.235	0.164	0.726
Present case 3	140	728000	1.340	0.232	0.164	0.725
Williamson (1989)	Exp.		—	—	0.164	—
Henderson (1995)	Exp.		—	—	—	0.73
Park (1998)	Num.		1.33	0.33	0.165	0.74
Zhang & Dalton (1998)	Num. 3D		1.32	0.23	—	—
Sharman et al. (2005)	Num. 2D		1.33	0.23	0.164	0.72

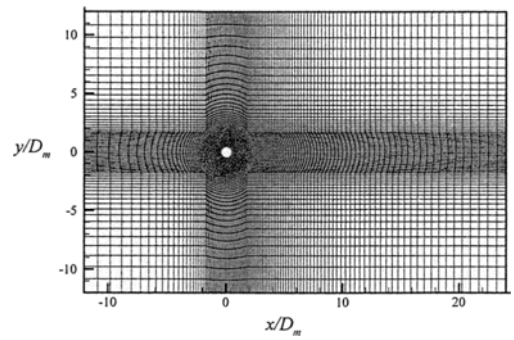

Fig. 2. Computational mesh for wavy cylinder on the x-y plane.

For computation, the flow domain is divided into a number of unstructured hexahedral grids. The gird is nonuniform on the x-y plane but uniform along the z direction. As shown in Fig. 2, the gird is clustered near the cylinder and the spacing is increased in a proper ratio away from the cylinder on the x-y plane. The accuracy of computational results is highly dependent on the mesh size and cell numbers. The results of grid test calculations are shown in Table 1. There are three test cases are constructed with the mesh numbers set to 100, 120 and 140 around the cylinder circumference, respectively. The height of spanwise direction (z-direction) is set to 6 D_m. The uniform layers of 64 are used along the z-direction. Compared with the experimental and numerical results of the circular cylinder at Re=100, the mean drag coefficient $\bar{C}_D$, the fluctuating lift coefficient C_L', the Strouhal number St and the base pressure coefficient C_{pb} are all consistent with the results of experimental and numerical results (Williamson, 1989; Henderson, 1995; Park et al., 1998; Zhang and Dalton, 1998; Sharman et al., 2005). In present calculations, the gird numbers base on the grid size of case 2 is adopted to calculate all the wavy cylinder cases. All of the present simulations are carried out with a fixed nondimensional time step $\Delta t = tU_\infty / D_m$ = 0025. Further more, the spanwise height of the computational domain is equal to one wavelength "λ" of the wavy cylinder. Tests are also performed with two, three and four wavelengths but don't show any difference in the forces and wake topology. So that only one wavelength height is chosen for the case of saving the computational time.

4. Results and discussions

For the wavy cylinders, a series of computational investigations have been carried out at a Reynolds number of 100 for different values of a/D_m and λ/D_m. All these investigations were compared with a circular cylinder at the same Reynolds number. To study the effect of variation of λ/D_m, the time histories

of the drag and lift coefficient are shown in Fig. 3. Compared with a circular cylinder, it can be clearly seen that the drag coefficient decreases sharply with increasing the value of wavelength for λ/D_m<5, while increases with the increasing the values of wavelength for λ/D_m>7. In the range of λ/D_m=5 to 7, the drag coefficient reaches a minimum value. This result is similar to the case of the wavy square cylinder at the same Reynolds number (Dareker and Sherwin, 2001). The lift coefficients of wavy cylinders are also suppressed corresponding with the drag reduction. In the range of λ/D_m=5 to 7, the lift fluctuations are close to zero. Hence, the optimal value of λ/D_m for drag reduction is in the range of λ/D_m=5 to 7.

Apart from the effect of different λ/D_m, the wavy amplitude a/D_m also plays an important role in drag reduction. As shown in Fig. 4, the time histories of drag and lift coefficients of the wavy cylinders were obtained. By increasing in the amplitude of the waviness a/D_m, both the drag coefficient and lift fluctuation of wavy cylinder are also reduced. Further the rate of reduction of drag coefficient becomes slow

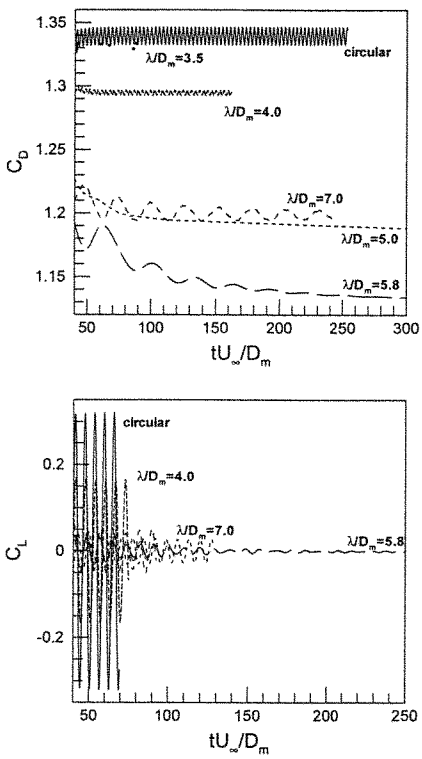

Fig. 3. Variation time histories of the drag and lift coefficients for wavy cylinders with different values of λ/D_m at a/D_m = 0.1.

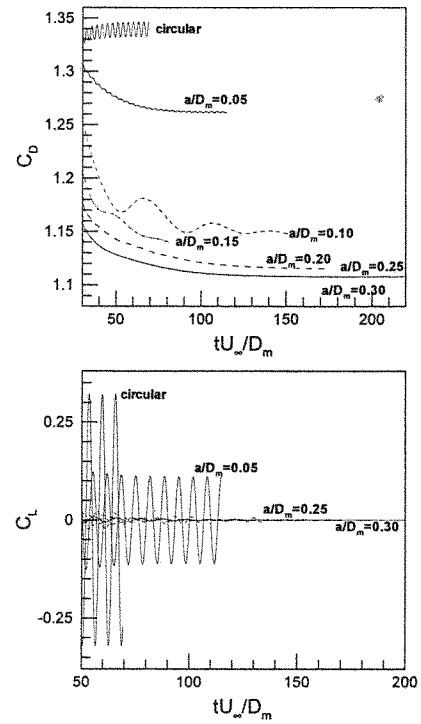

Fig. 4. Variation time histories of the drag and lift coefficients for wavy cylinders with different values of a/D_m at λ/D_m = 5.5.

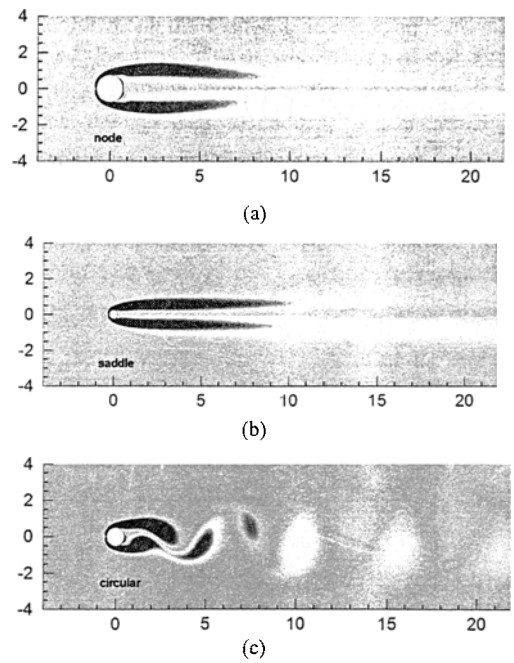

Fig. 5. The contours of instantaneous spanwise vorticity of the wavy cylinder at nodal (a) and saddle plane (b) compared with a circular cylinder (c) at Re=100, λ/D_m =5.5, a/D_m=0.25.

when a/D_m is greater than 0.1. At the range of a/D_m> 0.25, the fluctuating lift forces are close to zero.

To investigate the reasons of drag reduction, the instantaneous spanwise vorticity of the wavy cylinder (λ/D_m=5.5, a/D_m=0.25) at both nodal and saddle planes are shown in Fig. 5 compared with that of a circular cylinder. It is evident to find that the flow is steady and a pair of symmetric vortices forms in the near wake of the wavy cylinder, while for circular cylinder, the periodic Kármán vortex shedding behind the cylinder is observed. At the saddle plane of the wavy cylinder, the wake width is different from that of the nodal plane. This kind of wavy surface generates a three-dimensional vortex sheet which significantly modifies the near wake vortex structures. Such 3-D vortex sheet is more difficult to roll up into vortex. As a result, it rolls up into mature 3-D vortex at further downstream giving rise to a longer formation length. The transformation of the two-dimensional vortex sheet into three-dimensional vortex sheet strongly control the three-dimensional vortices formed in the near-wake of the wavy cylinder. Such is the physical reason behind the effect of the drag coefficient reduction and suppression of the FIV.

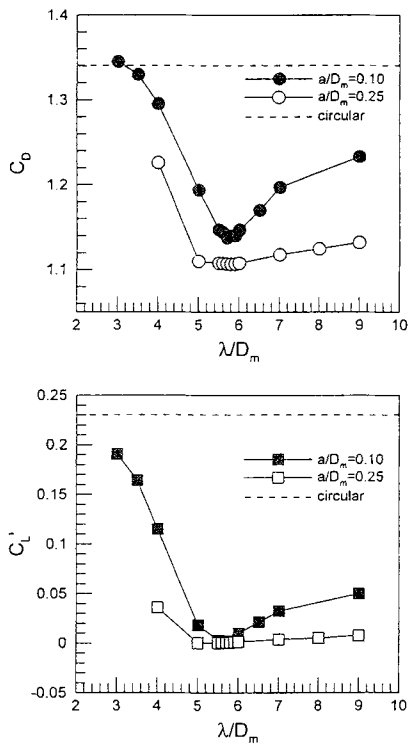

Fig. 6. Mean drag coefficients and fluctuating lift coefficients of wavy cylinders compared with a circular cylinder at Re=100.

The results for the variation of the mean drag coefficient and fluctuating lift coefficient with respect to the wave length λ/D_m and wave amplitude a/D_m are summarized in Fig. 6. The amplitude of lift fluctuations decreases as the drag efficient decreases. When the values of wavelength λ/D_m are from 5.5 to 6.0, the fluctuating lift coefficient approaches zero and and the periodic shedding is completely suppressed. At the range of λ/D_m < 5.5, the mean drag coefficient decreases quickly with increase in the value of λ/D_m and so is the fluctuating lift coefficient. However, the mean drag coefficients and fluctuating lift coefficient increased with the increasing for λ/D_m at the range of λ/D_m > 6.0. So the optimal range is between 5.5 and 6.0. Furthermore, it can be seen that the effect of λ/D_m for the drag reduction become smaller with the increase in a/D_m. The maximum mean drag coefficient reduction of the wavy cylinder up to 18% is obtained at the range of λ/D_m =5.5-6.0 for a fixed value of a/D_m =0.25 and the value of fluctuating lift coefficients are close to zero.

From the discussion above, the instantaneous vortex structures or the development of the vortex sheets are shown in Fig. 7. At λ/D_m=3 [Fig. 7(a)] the vortices have waviness due to the wavy structures, but the basic structures are not too much different from the normal two-dimensional vortex shedding of the circular cylinder [Fig. 7(f)]. For the case of λ/D_m=5.5, however, the wake structure is significantly deformed and periodic shedding process is completely suppressed [Fig. 7(c, h)]. At λ/D_m=4, 7 and 9 [Fig. 7(b, d, e, g, i, j)], the wake returns to an unsteady periodic state at further downstream. We can see that the structures of them are more complicated than for the cases of λ/D_m=3 and λ/D_m=5.5. It is believed that there exists an intrinsic preference of the spanwise wavelength significantly affects the natural flow structure when it matches the preferred wavelength. Furthermore, the wake formation lengths of some typical wavy cylinders are larger than that of the circular cylinder and little shedding appeared.

The range of λ/D_m =5.5-6.0 is little bigger than the mode-A wavelength of circular cylinders, it suggests that a wavelength which close to the mode-A wavelength of circular cylinders can suppress even prevent the Kármán vortex shedding. It also explains that why the cylinders with certain spanwise waviness could have a significant effect on the drag reduction and a corresponding suppression of cylinders vibration.

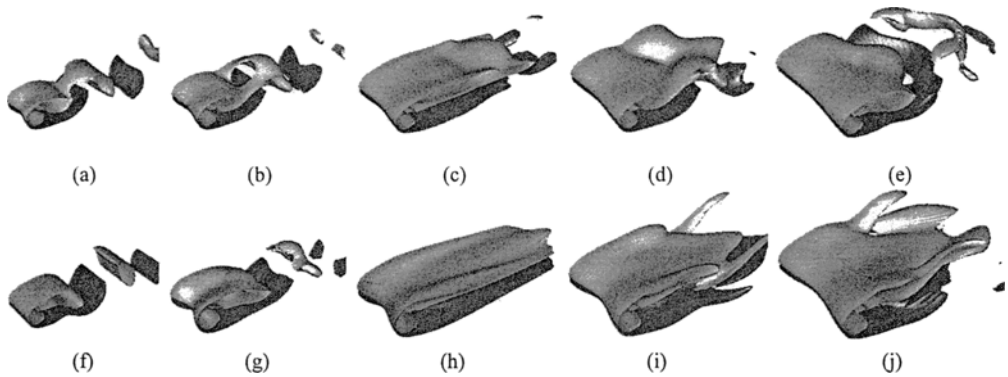

Fig. 7. Instantaneous spanwise vortex structures with different values of λ/D_m and a/D_m compared with a circular cylinder at Re=100. (a-e) λ/D_m equal to 3, 4, 5.5, 7, 9 respectively with a/D_m of 0.1; (f) circular cylinder; (g-j) λ/D_m equal to 4, 5.5, 7, 9 respectively with a/D_m of 0.25.

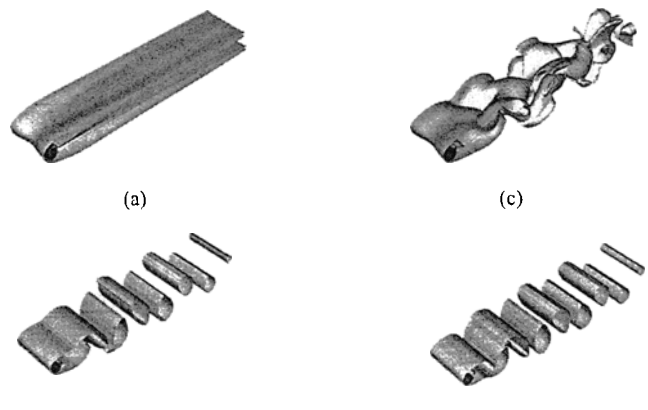

Fig. 8. Instantaneous vortex structures of wavy (λ/D_m =6, a/D_m=0.15) and circular cylinder at Re=100 (a, b) and Re=150 (c,d), respectively.

Furthermore, the vortex patterns of the typical wavy cylinder model (λ/D_m =6, a/D_m=0.15) and a circular cylinder model at Re=150 are shown in Fig.8. Compared with the wake pattern of wavy cylinder at Re=100, the complicated three-dimensional vortex structures appear at Re=150 [Fig. 8(c)]. From this figure, we can conclude that the vibration control by modifying the spanwise wavelength of the cylinder has a relationship with the variation of Reynolds number.

5. Conclusions

In present investigation, the main three-dimensional numerical simulations were used to calculate the laminar cross flow around wavy cylinders with different values of λ/D_m and a/D_m at Re=100. It was found that, this kind of wavy surface with some typical values of λ/D_m and a/D_m can significantly modify the free shear layer development and control the three-dimensional vortices formed behind the wake cylinder. As a result, it weakens the vortex shedding behind the wavy cylinders and increases the base pressure of the cylinder. The mean drag coefficients of the wavy cylinders are less than that of a corresponding circular cylinder, and the fluctuating lift coefficients are suppressed. The simulations explain why the cylinders with certain spanwise waviness could have a significant effect on drag reduction and a corresponding suppression of cylinders vibration. Furthermore, the optimal range of the wavelength was found to be at λ/D_m =5.5-6.0, which would give the greatest effects in drag reduction and FIV suppression. At this range, the maximum mean drag coefficient reduction of the wavy cylinder is up to 18% for a constant value of a/D_m=0.25 and the value of fluctuating lift coefficient is close to zero. It suggests that a wavy length which

close to the mode-A wavelength of circular cylinders can suppress even prevent the Kármán vortex shedding. Furthermore, the wavy cylinder with a large value of a/D_m can result in bigger drag reduction and suppression of the fluctuating lift. Furthermore, a typical wavy cylinder model at Re=150 was also simulated. And found that the flow induced vibration control by modifying the spanwise wavelength of the cylinder has a relationship with the variation of Reynolds number. All the results above explained why some cylinders with certain spanwise waviness and wavy amplitude could have a significant drag reduction and suppression of fluctuating lift coefficient for the prevention of the cylinder vibration.

Acknowledgements

The authors wish to thank the Research Grants Council of the Hong Kong Special Administrative Region, China, for its support through Grant No. PolyU 5311/04E.

References

Ahmed, A. and Bays-Muchmore, B., 1992, "Transverse Flow over a wavy Cylinder," *Physics of fluids A 4*, pp. 1959~1967.

Ahmed, A., Khan, M. J. and Bays-Muchmore, B., 1993, "Experimental Investigation of a Three-Dimensional Bluff-body wake," *AIAA Journal*, Vol. 31, pp. 559~563.

Bearman, P. W. and Owen, J. C., 1998, "Suppressing Vortex Shedding from Bluff Bodies by the Introduction of Wavy Separation Lines," *Proceedings of the 1998 ASME Fluids Engineering Division Summer Meeting*, FED-Vol. 245, Session 191-09, FEDSM98-5190, Washington, D. C.

Darekar, R. M. and Sherwin, S. J., 2001, "Flow past a Square-section Cylinder with a Wavy Stagnation Face," *Journal of Fluids Mechanics*, Vol. 426, pp. 263~295.

Henderson, R. D., 1995, "Details of the Drag Curve near the Onset of Vortex Shedding," *Physics of Fluids*, Vol. 7, pp. 2102~2104.

Lam, K., Wang, F. H., Li, J. Y. and So, R. M. C., 2004, "Experimental Investigation of the Mean and Fluctuating Forces of wavy (varicose) Cylinders in a Cross-flow," *Journal of Fluids and Sturcutres*, Vol. 19, pp. 321~334.

Lam, K., Wang, F. H. and So, R. M. C., 2004, "Three-Dimensional Nature of Vortices in the Near Wake of a Wavy Cylinder," *Journal of Fluids and Strucutres*, Vol. 19, pp. 815~833.

Nguyen, A. T. and Jee, S. J., 2004, "Experimental Investigation on Wake behind a Sinusoidal Cylinder," *Proceeding of Tenth Asian Congress of Fluid Mechanics*, Peradeniya, Sri Lanka.

Owen, J. C. and Bearman, P. W., 2001, "Passive Control of VIV with Drag Reduction," *Journal of Fluids and Structures*, Vol. 15, pp. 597~605.

Owen, J. C., Szewczyk, A. A. and Bearman, P. W. 2000, "Suppression of Kármán Vortex Shedding," *Gallery of Fluid Motion. Physics of Fluids*, Vol. 12, pp. 1~13.

Park, J., Kwon, K. and Choi, H., 1998, "Numerical Solutions of Flow Past a Circular Cylinder at Reynolds Number up to 160," *KSME International Journal*, Vol. 12, p. 1200.

Sharman, B., Lien, F.S, Davidson, L. and Norberg, C., 2005, "Numerical Predictions of Low Reynolds Number Flows over Two Tandem Circular Cylinders," *International Journal for Numerical Methods in Fluids*, Vol. 47, pp. 423~447.

Tombazis, N. and Bearman, P. W., 1997. "A Study of Three-dimensional Aspects of Vortex Shedding from a Bluff Body with a Mild Geometric Disturbance." *Journal of Fluid Mechanics*, Vol. 330, pp. 85~112.

Williamson, C. H. K., 1989, "Oblique and Parallel Modes of Vortex Shedding in the wake of a Circular Cylinder at Low Reynolds Numbers," *Journal of Fluid Mechanics*, Vol. 206, pp. 579~627.

Zhang, J. F. and Dalton, C., 1998, "A Three-Dimensional Simulation of a Steady Approach flow past a Circular Cylinder at Low Reynolds Number," *International Journal for Numerical Methods in Fluids*, Vol. 26, pp. 1003~1022.

Zhang, W., Dai, C. and Lee, S. J., 2005, "PIV Measurements of the Near-wake behind a Sinusoidal Cylinder," *Experiments in Fluids*, Vol. 38, pp. 824~832.